

# EFFECTS OF $V_2O_5$ AND NiO DOPANTS ON ZnO VARISTOR SYSTEM

I. O. OWATE and B. OTOKUNEFOR

(Received 6 August 1999; Revision accepted 2 December 1999)

## ABSTRACT.

The effects of  $V_2O_5$  and NiO dopants upon an established ZnO varistor system ( $ZnO-Bi_2O_3-CrO_3-MnO_2-Co_3O$ ) have been investigated. The system was processed and fabricated by the usual ceramic processing techniques. These involved ball milling, mixing, cold pressing and sintering. A set of the processed powders were doped with 0.1, 0.3, 0.5, 0.8 and 1.0 wt % of  $V_2O_5$  whilst another set was equally doped with the same proportion of NiO.

The final products were physically and electrically characterized. Factors such as the non-linearity factor, energy handling capacity and non-linear resistivity were estimated. It was generally observed that a concentration of about 0.1 wt %  $V_2O_5$  (dopant) expressed positive influence upon the characteristics of the system. The values of the non-linearity factor, barrier voltage, energy handling capacity and non-linear resistivity were  $65$ ,  $210 \times 10^4$  V/mm,  $387$  J/mm<sup>2</sup> and  $2362$  ohms-cm respectively. These values are considered relatively very good and equally compare favourably with previous work. It suffices to state that the effect of  $V_2O_5$  and NiO dopants on a typical varistor system have in part been established and improved upon.

**KEY WORDS:** ZnO, varistor, Effects, Dopants and Processing.

## INTRODUCTION

Zinc oxide varistor is a non-ohmic ceramic device characterized by low conductivity below its breakdown voltage (Asokan et al 1988). They are generally classified as ceramic semi-conductors with low level conductivity. The device consists mainly of ZnO (80 – 95 wt %). Other oxides such as  $Bi_2O_3$ ,  $MnO_2$  and  $SbO_2$  are usually added to the major system to give it special characteristics {Matsuoka(1971), Levinsion et al (1986) and Gupta(1990)}. The device fabricated from the above composition is capable of responding to both alternating and direct currents as well fast and short pulses {Bui et al (1989), Carlson et al (1982) and Clark (1989)}. In most cases the applied voltages are below the established threshold voltage of the system to be protected. The electrical characteristics of the varistor composite materials may be regarded as being similar to that of a double layer back-to-back Zener diodes with symmetric current-voltage {Bai (1992), Eva et al (1993) and Debashis et al (1992)}.

Different compositions of ZnO varistors have been designed, fabricated and prepared for several application purposes {Asokan et

al (1987), Carlson et al (1982) and Kimora et al (1989)}. Hence, it can be rightly stated that ZnO varistors are increasingly becoming accepted for protecting electrical and electronic devices from transient power surges and spikes. These problems usually occur in both domestic and industrial power lines due to lightning and abrupt discharges as well as sudden power changes. It is a common knowledge that sudden discharges and spikes arising from such changes in power supply are very dangerous to most electrical and electronic equipment. Observation shows that such effects have resulted to costly damages in refrigerators, laboratory instruments, musical and television sets {Mahan et al (1979) and Hower et al (1979)}.

In some cases, the discharges and spikes can occur without any previous warning. The rapid response time (within 50 nanoseconds) for the ZnO varistor, makes it an excellent circuit component and a good device protector (Gupta, 1990) that could provide the desired energy discharge capability. Similarly, the disk of the varistor is usually placed in a porcelain enclosure, which provides support, acts as heat

removal system and as seal for isolations of contamination within the electrical environment.

System over-voltage that may cause voltage surges could arise from either internally or externally generated process. Such processes include lightning and sudden switching on or off of devices. It should be known that the arrester does not determine the origin of the over-voltage but rather attempts to limit the magnitude of all abnormal voltages above the specified values. This is why ZnO varistor are normally connected directly across the power line and in parallel with the load to be protected. The consideration of both the equipment and varistor's rating is very paramount in the above stated process. By virtue of the fact that most varistors are ceramics, they can be fabricated into a variety of sizes and shapes due to the available and well established ceramic processing techniques. This facilitates its high degree of flexibility and adaptation. Fabrication of ZnO varistor is usually achieved through the combination of processing techniques. These include compaction and sintering processes between 1,100 to 1,300 °C (Hawer et al, 1979). These processes include doping at the correct time, controlling grain growth and the sintering temperature (Jimei et al (1995), Senda et al (1990), Sung et al (1991) and Shr-Nan et al (1993)).

The present work investigates the effects of dopants and sintering at low temperature while controlling other factors on a standard ZnO varistor composition system. It is expected that such changes might produce an efficient varistor material with improved characteristics.

### THEORY

A typical ZnO varistor system consists of a microstructure whose conducting grains (ZnO) are surrounded by a very thin layer (about 0.001  $\mu\text{m}$ ) of insulating materials such as Bi, Ni and Nb<sub>2</sub>O<sub>5</sub> that segregate to the grain boundary (Asokan, 1987). Thus, there are three distinct phases; the ZnO grains, intergranular and the particles or spinel regions. This is schematically shown in Figures 1 and 2.

It means that the ZnO conducting grains are surrounded by an electrically insulation layer of Bi<sub>2</sub>O<sub>3</sub> phases. Schottky barriers are formed within the grain boundaries containing the Bi<sub>2</sub>O<sub>3</sub> phases and this is

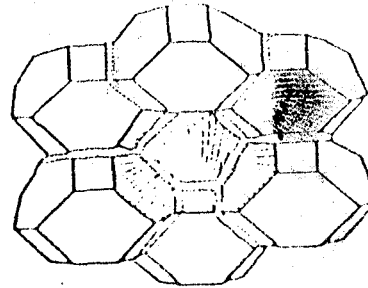


Fig. 1 Schematic representation of The ZnO Varistor.

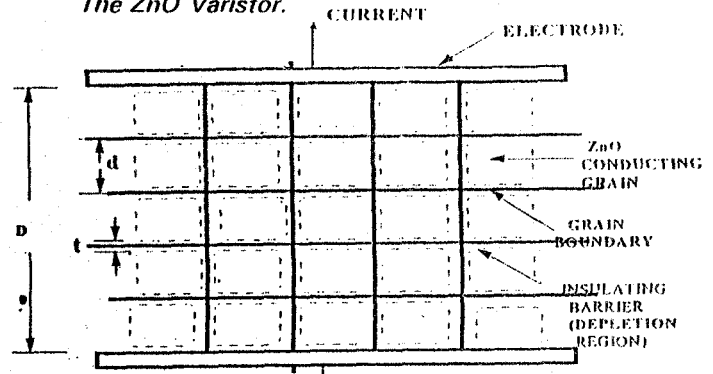


Fig. 2 A block diagram model of a varistor Varistor system.

usually responsible for the non-ohmic properties of most devices made from ZnO varistors. Various additives influence the concentration of Bi<sub>2</sub>O<sub>3</sub> in the varistor system after the sintering process. This could in part be due to evaporation of the material and it is against this background that Bi<sub>2</sub>O<sub>3</sub> is normally added in different proportions as a dopant to ascertain overall effect on the ZnO varistor. Its effect is in part due to the movement of negative charges, (mainly electrons) across several ZnO grains and grain boundaries that act as the barriers to electrical conduction (Kimora, 1989). It has been reported (Bai, 1992) that electrical conduction in ZnO varistors occurs through the process of direct surface migration of charges resulting in the development of current and voltage

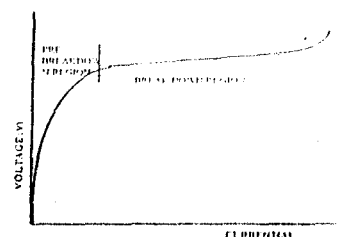


Fig. 3 A typical I-V characteristics of a Varistor.

across bulk material and grain boundaries. A typical current-voltage characteristic (Figure

3) is symmetrical and similar to that of that of a back-to-back Zener diode. Regions of pre-breakdown and upturn are commonly identified. The current relationship within the pre-breakdown region depends upon the thermal process and can be mathematically presented as (Eda, 1978),

$$I = I_0 \exp\{\theta/kT\} \dots\dots\dots(1)$$

$\theta = 0.6 - 0.9$  at 280 K

T = Temperature in K

k = Boltzmann's constant

I = Final current

I<sub>0</sub> = Initial current

Within the breakdown region, the current density becomes virtually independent of the temperature and is represented by the equation (Debashis et al, 1992);

$$\frac{J_1}{J_2} = \left(\frac{E_1}{E_2}\right)^\alpha \dots\dots\dots(2)$$

where  $\alpha = \text{nonlinearity constant}$

J<sub>1</sub>, J<sub>2</sub> are current densities and E<sub>1</sub>, E<sub>2</sub> are the field strengths. The leakage current of the samples (15-mm diameter and 1-mm thickness) was estimated at 80% of the pre-breakdown voltage. Thus the non-linearity factor and non-linear resistivity could be calculated by using values derived from the graphs which were obtained on the basis of equation 2. The equation may be written as;

$$\text{Log} J_1 - \text{Log} J_2 = 1/\alpha (\text{Log} E_1 - \text{Log} E_2) \dots\dots\dots(3)$$

**EXPERIMENTAL TECHNIQUES**

The fabrication of the ZnO varistor followed the usual conventional ceramic techniques. This involved weighing of specimen, mixing, pressing and sintering. High purity ZnO, Bi<sub>2</sub>O<sub>3</sub>, Co<sub>3</sub>O<sub>4</sub>, MnO<sub>2</sub> and V<sub>2</sub>O<sub>5</sub> (99.99% purity) were weighed out in relative proportions to produce five samples that differed only in NiO and V<sub>2</sub>O<sub>5</sub> (minute

fraction) concentrations. The weight percentages of the major components are presented in Table 1. The major components were later doped with both the Vanadium oxide and the Nickel oxide in the varying proportion of 0.1, 0.3, 0.5, 0.8 and 1.0 wt % respectively to produce the samples that were studied. Five specimens doped with V<sub>2</sub>O<sub>5</sub> and another five doped with NiO were achieved. Each sample was thoroughly mixed using mortar and pestle for 15 minutes and transferred into a plastic vessel containing some de-ionized water for further processing using a motorized vibrator. The system was electrically vibrated at maximum

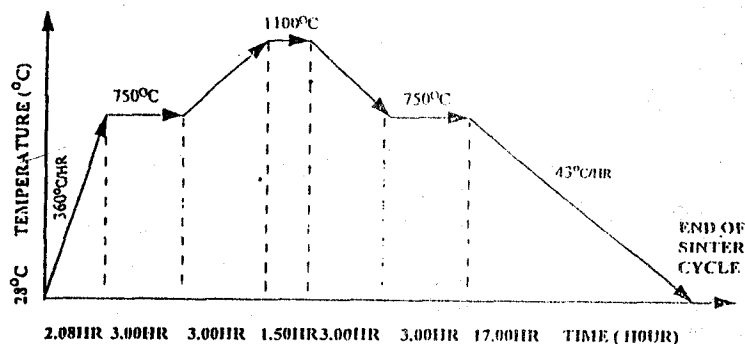


Fig.4 The sintering Cycle of the system.

speed for four hours. The resulting homogeneous mixture was dried at 200°C in an oven and then calcined at 750°C for 20 minutes. The calcined samples were cooled to room temperature (35°C), crushed and grounded using mortar pestle and then dried. Disc-shaped pellet samples of diameter 10.00 mm and thickness 1.00 mm were then formed using a hydraulic press at 112 N/mm<sup>2</sup> pressure. The thickness and diameter of samples were measured using a micrometer screw gauge. The resulting green densities were estimated and then the samples were sintered by heating the specimens from room temperature (35°C) to 750°C at the rate of 360°C/hr. This temperature was maintained for three hours in order to burn off the binder. The temperature was then increased to 1000°C at 83°C/hr and held for another 1 hour 30 minutes. The system was later cooled at the rate of 83°C/hr until it attained a temperature of 750°C. Thereafter, it was reduced to 35°C at the rate of 45°C/hr. A typical sintering cycle described is presented in Fig.4. The two surfaces of the

Table 1: Concentrations of major varistor components

Major Components.	Weights of components (wt %)
ZnO	91.01
Bi <sub>2</sub> O <sub>3</sub>	7.02
CrO <sub>3</sub>	0.50
MnO <sub>2</sub>	0.50
Co <sub>3</sub> O <sub>4</sub>	0.50

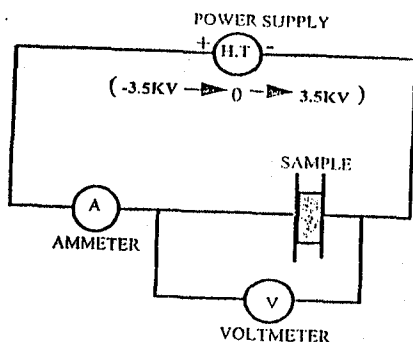


Fig.5 Electrical circuit for the measurement.

samples were coated with conductive silver paint (produced by Chemtronic Inc Kennesaw, U.S.A.) after which electrodes were attached and current-voltage measurements were performed using an ammeter, voltmeter and a high-tension power supply unit (Fig.5). Measurements were also performed using LCR meter applying four test frequencies of 50 Hz, 10 kHz, 20 kHz and 30 kHz.

### RESULTS AND DISCUSSIONS.

Table 2 shows the green, measured and theoretical densities of the samples with respect to densification percentage, mean weight losses and the weight percent of the dopants. It was observed that samples containing  $V_2O_5$  as the dopant exhibited a decrease in weight loss with increasing concentration of  $V_2O_5$ . This behaviour is not attributable to moisture loss of the dopant via evaporation process because the quantitative value of weight loss at lower dopant concentrations were relatively more than the concentration of the additive-dopants. Beside, if the dopant were reduced by evaporation process, the quantity lost should be reflected by the relative quantity of the additive-dopant, since the melting point of the parent material is higher than

the sintering temperature. However, it could be deduced that the addition of  $V_2O_5$  from 0.1 to 1.0 wt % levels reduced the volatilization of the oxides hence the reduction in weight loss with increasing concentration of  $V_2O_5$  for the samples. In contrast samples containing NiO (dopant) did not indicate similar behaviour. Weight loss

NiO dopant was expected since its melting point is about  $1914^\circ\text{C}$  and the system was sintered at  $1150^\circ\text{C}$ . Also, high degree of densification was achieved for samples doped with  $V_2O_5$ . In particular, specimen with 0.1 wt %  $V_2O_5$  produced 97% densification whereas samples doped with similar concentrations of NiO yielded an average of 92.76% densification. Again, this appears low for the application characteristics required. Thus, the densification process could be described (Table 2) as fairly constant for the NiO dopant. Despite the observed relative losses in weight, constant densification pre-supposes changes in volume of specimens with respect to mass of compressed samples due to the reduction in volatility. This further suggests that the ratio of change in mass to change in volume is constant. In addition, increases in volume could be credited to resulting chemical changes, which usually generated larger ionic radii species from some of the dopants. It has earlier been reported (Vanadamme, 1980) that  $V^{5+}$  which had an ionic radius of 0.059 nm and a reduction state of  $V^{2+}$  has the characteristic of increasing in ionic radius during the sintering process. By and large, changes in ionic states of the dopants used will partly be prominent in Bismuth oxide as reported by Asokan (1987).

Table 2. The densification process and percentage weight loss of samples

Dopants (WT %)	DENSITIES OF SAMPLES ( $\text{g}/\text{cm}^3$ )						DENSIFICATION (%)		WEIGHT LOSS (%)	
	Green		Measured		Theoretical.					
	$V_2O_3$	NiO	$V_2O_3$	NiO	$V_2O_3$	NiO	$V_2O_3$	NiO	$V_2O_3$	NiO
0.1	5.04	4.99	5.69	5.42	5.80	5.80	98.05	93.50	2.47	1.42
0.3	5.10	5.00	5.60	5.40	5.79	5.80	96.70	95.01	1.43	1.46
0.5	5.02	4.97	5.45	5.31	5.79	5.80	94.10	92.00	0.32	1.33
0.8	4.92	4.95	5.50	5.36	5.78	5.81	95.30	92.03	0.86	1.45
1.0	4.97	5.07	5.65	5.41	5.78	5.81	96.60	93.00	0.04	1.35

at various levels of dopant (NiO) which could be averaged to a constant concentration exhibited irregular pattern, variation. This characteristic behaviour for

Consequently, the surface state density of the samples with high concentration of V<sub>2</sub>O<sub>5</sub> was higher than that of others. This could be attributed to a decrease in grain boundary areas as a result of grain growth. Thus the barrier voltage increased with increasing V<sub>2</sub>O<sub>5</sub> content. It then implies that some V<sup>2+</sup> ions migrated to the grain boundary region and influenced the charge distribution pattern. This might have increased the width of the barrier voltage in an irregular fashion. The plots of the field strengths as a function of current density for both dopants are presented in figures 6 and 7.

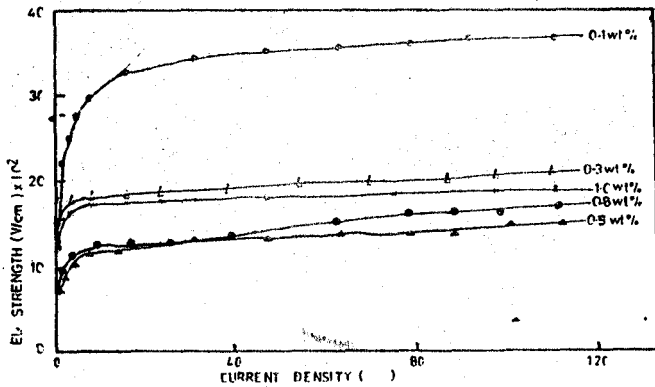


Fig.6 The Field strength Vs Current density for samples containing V<sub>2</sub>O<sub>5</sub>.

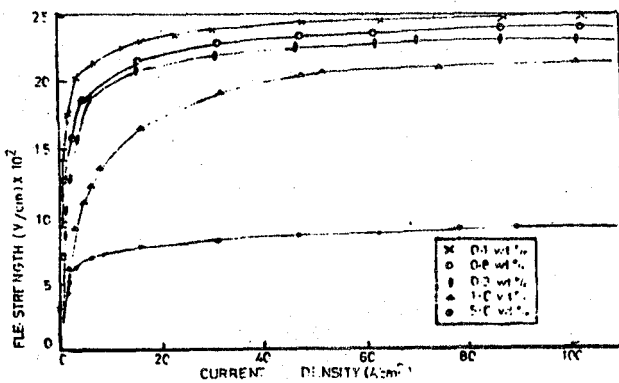


Fig.7 The field strength Vs Current density for samples containing NiO.

These are equivalent to the voltage-current characteristics as they present the same information. Thus it may be observed that better characteristics were obtained for low level addition (0.1 wt %) of V<sub>2</sub>O<sub>5</sub> as the leakage current is lower than at high V<sub>2</sub>O<sub>5</sub> concentrations. In contrast, the voltage-current characteristics of the samples containing NiO were less stable and the leakage current relatively high.

The other parameters that could determine the suitability of the sample's compositions as a varistor material were calculated using technique adopted by Asokan et al (1987) and presented in Table 3. These include the non-linearity factor, non-linear resistivity, energy handling capacity and energy barrier voltages. It is significant to report that Table 3 shows that only one compositional system (sample doped with 0.1 wt %) exhibited good varistor characteristics. Its non-linearity factor agrees with the I-V characteristic pattern obtained by Levinson (1986) and Asokan et al (1987) for varistor systems. But this deteriorated as V<sub>2</sub>O<sub>5</sub> content increases. For example V<sub>2</sub>O<sub>5</sub> content of 0.1 wt % produced  $\alpha = 65$ , whereas for V<sub>2</sub>O<sub>5</sub> of 1.0 wt % it recorded  $\alpha = 15$ . Similarly non-linear resistivity for 0.1 wt % of V<sub>2</sub>O<sub>5</sub> was 2362  $\Omega$ -cm but only 1134  $\Omega$ -cm at 1 wt % of V<sub>2</sub>O<sub>5</sub>. The other parameters followed similar trends or patterns, whereas the NiO-doped systems showed irregular patterns. Other researchers; Eda (1978), Morris (1976) and Eva et al (1993) have equally shown that products made via controlled routes usually yield good results. A non-linearity factor of about 50 and a breakdown voltage of  $1 \times 10^5$  V/mm with an energy handling capacity of 300 J/mm<sup>3</sup> have been achieved at a sintering temperature of 1230°C by Vanadamme (1980). This temperature is rather high. It suffices to state that the effects of V<sub>2</sub>O<sub>5</sub> and NiO dopants on the varistor system have in part been established and that V<sub>2</sub>O<sub>5</sub> (in small

Table 3. The measured characteristic parameters.

Dopants (wt %)	Non-linearity Factor ( $\alpha$ )		Non-linearity Resistivity ( $\Omega$ -cm)		Energy Barrier Voltage (eV/mm)		Energy handling Capacity (J/mm <sup>2</sup> )	
	V <sub>2</sub> O <sub>5</sub>	NiO	V <sub>2</sub> O <sub>5</sub>	NiO	V <sub>2</sub> O <sub>5</sub>	NiO	V <sub>2</sub> O <sub>5</sub>	NiO
0.1	65	23	2362	3970	210.42	1.77	287.06	26.79
0.3	17	14	2119	3905	17.50	1.60	135.42	23.90
0.5	15	14	2703	3009	111.65	2.34	141.25	34.51
0.8	19	17	2632	2795	112.28	1.90	136.22	26.02
1.0	15	10	1134	1504	81.04	13.11	133.21	43.59

quantity) enhances the quality of the varistor system.

### CONCLUSIONS.

The additions of  $V_2O_5$  and NiO to the ZnO- $Bi_2O_3$ - $CrO_3$ - $MnO_2$ - $Co_3O_4$  varistor system increased the grain resistivity of the product and other properties. This was responsible for the increase in energy handling capacity and the efficient non-linearity factor obtained. Consequently,  $V_2O_5$  showed good characteristics of a promising dopant for the current compositional system at a concentration of 0.1 wt %. NiO did not positively influence the varistor system that was investigated. At a small concentration of 0.1 wt %,  $V_2O_5$  dopant exhibited an outstanding non-linearity factor of 65, barrier voltage of  $210 \times 10^4$  V/mm, energy handling capacity of  $387 \text{ J/mm}^3$  and non-linear resistivity of  $2362 \text{ } \Omega\text{-cm}$ . These values are both comparatively and relatively good for a practical varistor system and there are the possibilities of using  $V_2O_5$  as volatility inhibitors.

### ACKNOWLEDGEMENT

The authors wish to acknowledge the roles played by Prof. Ebeniro, J. O; Mr. Ekeocha, C.C. and the department of Physics, University of Port Harcourt in providing materials and support instruments during the process of this work. Your efforts have in no small measure assisted in the production of the piece

### REFERENCES

- Asokan, T; Iyengar, G.N.K and Nagabhushana, G.R., 1987. Influence of process variation on the microstructure of ZnO-based non-linear resistors, *J. Am. Ceram. Soc.* 70: 643.
- Asokan, T; Iyengar, G.N.K. and Nagabhushana, G.R., 1988. Improvement of non-linear characteristics of ZnO based Ceramics, *IEEE Transactions on electrical insulation*, 23(2): 279 - 286.
- Bai, S.N. and Tseng, T.Y., 1992. ZnO characteristics *JPN. J. App. Physics*, 31:81 - 90.
- Bui, A and Hassanzadeh, A.L.M., 1989. Electrical characteristic degradation of ZnO varistor, *J. App. Physics* 65(10): 4048 - 4057.
- Carlson, W.G. and Gupta, T.K., 1982. Degradation mechanisms of non-ohmic ZnO. *J. App. Physics*. 53:5746 - 5749.
- Clark, D.R., 1989. Grain boundary segregation in a commercial ZnO varistor, *J. Am. Ceram. Bull.* 60: 6827.
- Debashis, D. and Bradth, R.C., 1992. Grain growth of ZnO during liquid phases sintering. *J. Am. Ceram. Soc.* 75(9): 2529 - 2534.
- Eda, K., 1978. Powder diffraction patterns of Bismuth Oxides, *J. Am. Ceram. Soc.* 6(11): 494.
- Eva, O; Dunlop, G. and Osterlund, R., 1993. Development of functional microstructure on sintering. *J. Am. Ceram. Soc.* 76(1): 65 - 71.
- Gupta T.K., 1990. Applications of ZnO Varistor. *J. Am. Ceram. Soc.* 73(3): 1817 - 1840.
- Hower, P.L. and Gupta, T.K; 1979. Admittance spectroscopy of ZnO. *J. App. Physics*, 50:4847.
- Jimeï, F. and Freer, R., 1995. The roles played by Ag and Al dopants in controlling the electrical properties of ZnO varistor. *J. App. Physics*, 77(9): 4795 - 4800.
- Kimra, J.K. and Yamaguchi, T.J., 1989. Effects of Bismuth oxide content on sintering of ZnO. *J. Am. Ceram. Soc.* 72(8): 1514 - 1544.
- Levinson, L. M. and Philip, H.R., 1986. ZnO varistors - A review; *Ceram. Bulletin*, 65(4): 639 - 647.
- Mahan, G. D. Levinson, L. M. and Philip, H. R., 1979. Theory of conduction in ZnO varistors. *J. App. Physics*, 50: 2799 - 2804.
- Matsuoka, M., 1971. The proto-type varistor and the market value. *JPN J. App. Physics* 10: 736 - 740.
- Morris, W. G., 1978. Surface properties of a coated ZnO varistor. *J. Vac. Sc. Tech.*; 13: 926 - 932.
- Senda, T. and Bradt, R. C., 1990. Grain growth in sintered ZnO- $Bi_2O_3$  ceramics. *J. Am. Ceram. Soc.* 3:106 - 114.
- Shr-Nan, B. and Tseung, T., 1993. Influence of sintering temperature on electrical properties of ZnO varistor. *J. App. Physics* 74(1):695 - 703.
- Sung-Chu, Y. and Randal, M. G., 1991. Grain growth kinetics in liquid phase sintered ZnO. *J. Am. Ceram. Soc.* 74(12): 3085 - 3090.
- Vanadamme, L. K. J. and Brugman, J. C., 1980. Conduction mechanisms in ZnO varistors. *J. App. Physics* 5(8):4240 - 4250.